

Purdue University

Purdue e-Pubs

International Refrigeration and Air Conditioning
Conference

School of Mechanical Engineering

2022

Design of Phase-change Thermal Storage Device in a Heat Pump for Building Electric Peak Load Shaving

Ransisi Huang

Allison Mahvi

Eric Kozubal

Jason Woods

Follow this and additional works at: <https://docs.lib.purdue.edu/iracc>

Huang, Ransisi; Mahvi, Allison; Kozubal, Eric; and Woods, Jason, "Design of Phase-change Thermal Storage Device in a Heat Pump for Building Electric Peak Load Shaving" (2022). *International Refrigeration and Air Conditioning Conference*. Paper 2299.
<https://docs.lib.purdue.edu/iracc/2299>

This document has been made available through Purdue e-Pubs, a service of the Purdue University Libraries. Please contact epubs@purdue.edu for additional information. Complete proceedings may be acquired in print and on CD-ROM directly from the Ray W. Herrick Laboratories at <https://engineering.purdue.edu/Herrick/Events/orderlit.html>

Design of A Phase-Change Thermal Storage Device in A Heat Pump for Building Electric Peak Load Shaving

Ransisi HUANG, Allison MAHVI, Eric KOZUBAL, Jason WOODS*

National Renewable Energy Laboratory, Building Technology Science Center
Golden, Colorado, United States

* Corresponding Author: jason.woods@nrel.gov

ABSTRACT

Replacing carbon-intensive fossil fuel heating systems with electric heat pumps powered by renewables is a promising approach to decarbonize the building sector. However, one of the technical barriers of this approach is the large scale of heat demand, which will put excessive stress on the electricity grid. Integrating thermal energy storage (TES) into the heating systems can help alleviate this problem, by shifting thermal load and thus shaving peaks in the building electric load. Therefore, it is critical to understand how to design a thermal storage device in a heat pump for peak load shaving.

In this study, we developed a numerical model for a cascaded vapor compression heat pump system integrating a phase change thermal storage device. This novel system can control the net thermal charging and discharging rate of the TES independently from the building's thermal load, which allows for precise control of electric power use. In the current study, we controlled the system to shave building electric peak load during a cold winter morning, and to charge TES during the relatively warm afternoon while still providing space heating. We used the model to evaluate the system performance with and without peak shaving. We also investigated the effect of PCM transition temperature on the peak reduction and electric energy saving potentials.

The results show that the peak shaving scheme effectively reduces the peak electric power consumption during a predefined discharge time window. When comparing to the no shaving case, for PCM with a transition temperature of 10 °C, the peak electric load reduction is 23.5%. When comparing to an air-source heat pump with back up electric resistance heater, as the transition temperature increases from 0 to 20 °C, the peak reduction increases from 46.1% to 50.9%. Integrating PCM with a transition temperature of 10 °C with peak shaving leads to the 45.5% of electric energy saving, which is the highest among the three transition temperatures.

Keywords: Thermal energy storage, PCM heat exchanger, Heat pump, Peak load shaving, Electric energy saving

1. INTRODUCTION

To tackle the climate crisis, the United States has embarked on an ambitious transition to a carbon-free energy economy by 2050. In 2015, CO₂ emissions from fossil fuel combustion to heat air or water in buildings contributed to 8.6% of total U.S. greenhouse gas emission (Leung, 2018). Therefore, it is evident that reducing the carbon emission associated with heating buildings is an essential element of the larger decarbonization goal. One potential technical path is to electrify heating systems: replace fossil fuel boilers with high efficiency electric heat pumps that are powered by renewable energy. However, many researchers have highlighted the concern that widespread heat pump adoption will inevitably increase buildings' peak electric demand above the supply capability of the current grid. For example, it is estimated that only 53% of U.S. space heating energy can be electrically driven without exceeding current peak electric loads (Waite & Modi, 2020). Another study suggests that full U.K. heating electrification could cause peak electric load to more than double (Cooper, Hammond, McManus, & Danny, 2016). To alleviate the load implication, thermal energy storage (TES) is a potential solution, by shifting thermal load and thus shaving peaks in the building electric load (Hutty, Patel, Dong, & Brown, 2020).

Thermal storage can be either sensible, latent or chemical. While sensible storage (e.g., water heating) is common and inexpensive, latent storage offers higher energy densities (>150 kJ kg⁻¹) that can be accessed within a small temperature band. These features lend themselves well to building HVAC&R applications (Moreno, Sole, Castell, &

Cabeza, 2014) (Sharif, et al., 2015) because they lead to compact components that can be efficiently integrated into vapor compression cycles. One challenge of using PCMs are their low thermal conductivity that hinders the heat transfer rate during charging or discharging (melting or solidifying). Therefore, many researchers are interested in how to design the PCM HX for specific requirements. Kuznik et al. developed a methodology based on dimensionless analysis to design air to PCM heat exchanger for the purpose of building peak load shaving (Kuznik, Lopez, Baillis, & Johannes, 2015). Hirmiz et al. proposed an analytical method to size PCM encapsulation for residential heat pumps (Hirmiz, Teamah, Lightstone, & Cotton, 2020).

We identified two limitations from the current work on leveraging PCM for building thermal load shifting. First, most existing design methods assume that PCM HX is subjected to simplified boundary conditions that somewhat reflect the system requirements, for example, discharge rate and system temperature differential. This expedites the design process but could limit the applicability of the results. Moreover, most current heat pump system configurations require temporary sacrifice of indoor thermal comfort while it handles outdoor coil defrosting.

Therefore, we propose a novel cascaded heat pump with integrated phase change thermal storage. The dual circuit configuration decouples meeting the building thermal load from thermally discharging or charging TES. Therefore, the integrated thermal storage acts as a thermal buffer that potentially enables defrosting while the system still provides space heating. In the current study, we control the system to shave electric peak load by utilizing the stored thermal energy in the PCM HX, and recharge TES when the weather condition favors the heat pump operation. We evaluated the load shifting performance of the proposed system over one individual day, and we assessed the impact of PCM T_i on the peak electric power reduction and electric energy consumption savings. For comparison purpose, we consider two baselines to calculate power reduction and energy savings. The first baseline is the same configuration without peak shaving, while the second baseline is a single stage, non-cascaded heat pump with a backup electric heater. The first baseline, which does not melt or freeze the TES during the modelled time-period, serves to benchmark the load shifting benefits of the integrated TES. The second baseline represents a typical option that may be installed today and serves to benchmark the energy saving potential of the full technology.

2. METHODS

2.1 TES integrated heat pump system description

Figure 1 shows a schematic of a R410A cascade heat pump system with integrated thermal storage. The system consists of a low-stage outdoor circuit and a high-stage indoor circuit thermally connected by a TES heat exchanger (TES HX). The low stage refrigerant from J2 thermally charges the storage device by condensing and releasing heat to the PCM, while the high stage refrigerant from J8 thermally discharges the device by evaporating and absorbing heat from PCM. The heat transfer dynamics among the low stage refrigerant, high stage refrigerant and TES will be detailed below. The refrigerant at J5 is then pumped by the high stage compressor to J6 as high pressure, high temperature vapor. It condenses in the heating coil while heating up the supply air to above 37 °C, and thus provides space heating to the building.

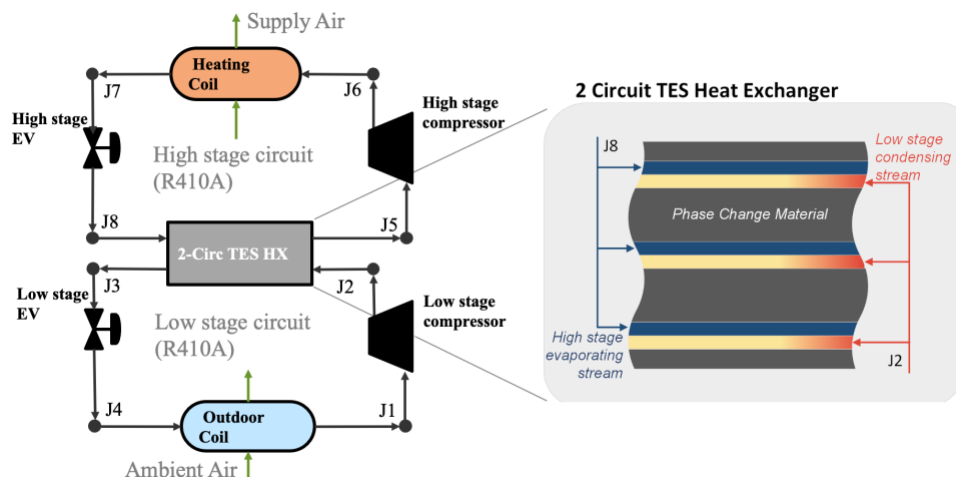


Figure 1: Schematic of thermal storage integrated cascade heat pump with a more detailed schematic of the TES HX.

The TES HX contains the low stage condensing refrigerant stream, the high stage evaporating refrigerant stream and the PCM that stores thermal energy. The refrigerant streams flow through multi-port extruded aluminum tubes, each of which are 1.2 m long, 0.25 m wide and contain 234 ports with a hydraulic diameter of 0.7 mm. These tubes are stacked directly on top of each other to ensure good thermal contact. Each channel pair is sandwiched between a composite material that contains a high thermal conductivity compressed graphite matrix impregnated with a PCM. This PCM composite has a net latent heat of 167 kJ/kg, a baseline transition temperature of 10°C, a density of 836 kg/m³, and a thermal conductivity of 10 W/m·K perpendicular to the compression direction. The thickness of the PCM composite material between each channel pair is 14.6 cm. The total energy capacity stored in the TES is 17.6 kWh, and the energy density is 39.1 kWh/m³. Table 1 summarizes the key parameters of the TES used for investigation. The PCM gives the system more flexibility by decoupling the condensing and evaporating heat transfer rates. For example, the system controller can reduce the refrigerant flow rate in the low stage circuit to decrease the compressor power. This reduces the low stage condensation heat transfer rate in the TES heat exchanger, which will then not match the high stage evaporating heat transfer rate needed to supply the room load. In this case, the PCM can supply the remaining heat to the evaporating stream by depleting its stored thermal energy. The heat is released as the cold refrigerant stream (high stage stream) solidifies the PCM material, which will discharge the TES heat exchanger over time. This process must eventually be reversed by increasing the capacity of the low stage circuit to melt the PCM and return it to a fully charged state. We define fully charged (state of charge, or $SOC = 100\%$) as an enthalpy state where the PCM is isothermal at 2 K above the transition temperature ($T = T_t + 2$) and fully discharged ($SOC = 0\%$) for isothermal PCM at $T = T_t - 2$.

Table 1: Key parameters of the TES heat exchanger

Key design and thermo-physical parameter	Value
Total energy capacity (kWh)	17.6
Dimensions (m)	$1.2 \times 0.25 \times 1.5$
Energy density (kWh/m ³)	39.1
PCM T_t (baseline)	10°C
Latent heat (kJ/kg)	167
Density (kg/m ³)	836

The system can operate the thermal storage device in three different modes while simultaneously providing space heating: net discharge mode, and net charge mode, and net zero C rate mode. For thermal storage, the C rate is the net discharging heat transfer rate divided by the maximum thermal energy capacity (kWh). In the net discharge mode, the high stage refrigerant discharges the TES heat exchanger faster than the low stage refrigerant charges the device. This mode is denoted by a positive C rate. In the net charge mode, the low stage refrigerant charges the device faster than the high stage refrigerant discharges the device and is denoted by a negative C rate. In the net zero C rate mode, the high stage and low stage refrigerants do not release or extract heat from PCM, so that the state of charge (SOC) of TES heat exchanger remains constant.

2.2 Component models and system solution approach

To reasonably simplify the system simulation, we make the following assumptions:

- Both expansion devices in the system are represented with an isenthalpic process
- Pressure drops in all the heat exchangers are neglected
- Power consumption associated with fans are neglected
- Compressor efficiencies are only a linear function of the compression ratio

We developed a quasi-steady state component-based simulation framework to simulate the single day system performance. The system was numerically represented as a network of components. Each component is a module on its own represented by a set of engineering equations or a performance map to predict the component steady-state performance under given inlet conditions. The two compressors are characterized with a volumetric efficiency and isentropic efficiency, both of which are assumed to be a linear function of the compression ratio (Hwang, 2004). The outdoor and heating coils are modeled with a three-zone approach (Huang, Ling, & Aute, Comparison of approximation-assisted heat exchanger models for steady-state simulation of vapor compression system, 2020) (also referred to as moving boundary approach), in which the heat exchanger is divided into two or three zones depending on the operating modes. Heat transfer in each zone is characterized by a lumped overall heat transfer coefficient. Finally, we used an approximation-assisted black-box model to represent the TES heat exchanger, which predicts the

refrigerant operating pressures required to deliver a specific evaporation and condensation heat transfer rate. The model is trained by MATLAB Deep Learning Toolbox using a detailed 2D transient finite-difference model like the model developed by Woods, et al., 2021. The detailed model discretizes the device into three types of nodes containing the PCM composite, refrigerant, and aluminum channel walls. The conduction heat transfer rates between PCM composite nodes are calculated with a discretized version of Fourier's law, accounting for directional differences in the thermal conductivity of the PCM composite. Heat transfer rates between different types of nodes are calculated by considering all relevant resistances, including fluid convection, contact, and conduction resistances. The model iteratively solves for the refrigerant pressures in each time instance so that the evaporating stream exits as a saturated vapor and the condensing stream reaches a saturated liquid state when it flows through 80% of the heat exchanger length, which will ensure some amount of refrigerant sub-cooling. The condensing stream convergence criteria (20% liquid length) was selected to keep the refrigerant charge relatively constant throughout each simulation.

We formulated a system of non-linear equations with the smallest possible set of variables that describe the steady state of the system. The detailed equation formulation method is adapted from the tripartite graph method (Huang, Aute, & Ling, 2021). These equations were then solved using quasi-Newton method (Dannis & Schnabel, 1996) to obtain the steady-state solution (refrigerant state points and PCM *SOC*) for each timestep. The system updates the PCM *SOC* before marching to the next time instance.

2.3 System control and operation method

The storage device alternates among the three modes (net discharge mode, net charge mode, and net zero C rate mode) to allow the system to shave electric peak load while meeting the thermal load of the indoor environment. We assume the thermal load variation on a typical winter day follows the profile in Figure 2(a). The corresponding ambient temperature profile is shown in Figure 2(b).

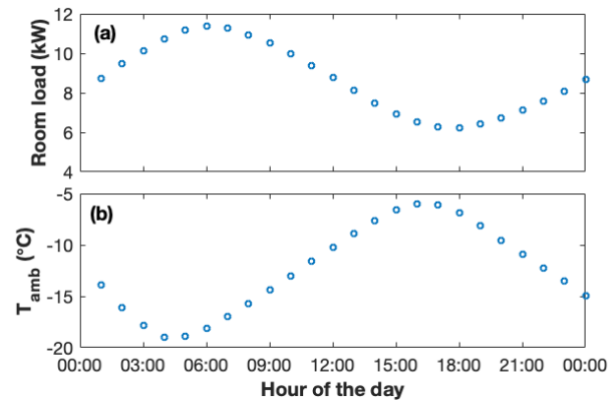


Figure 2: The (a) building load profile and (b) ambient temperature (T_{amb}) profile used for the 24-hour system simulation

We compared the performance of the system under two different control strategies. First, the system simply provided the building thermal load without temporally shifting any energy, meaning that the thermal storage heat exchanger was not thermally discharged or charged. The maximum total compressor power in this case is used as one of the baselines to define the peak electric power shaving fraction for the second control strategy. The second strategy aims to reduce the maximum electric power consumption during the discharge window, which we set as 3:00 to 9:00. The system in this window was operated at a minimal constant electric power while fully discharging the TES component, as to be shown in Figure 4 in section 3.1. The TES C rate is modulated to meet the peak shaving requirement. The TES heat exchanger was later regenerated by fully charging it at a constant power between 14:00 and 20:40 ($C_{rate} = -0.15$). Finally, we maintained the TES at a constant state of charge at all other times of the day ($C_{rate} = 0$). The system control variables during each of these operational stages is shown in Table 2.

Table 2: System peak shaving operation methods at different stages

Operation stage	TES mode	System controlled variables
Discharge window	Net discharge (positive C rate)	System capacity, total compressor power, TES C rate ranges between 0~0.25 1/h
Charge window	Net charge (negative C rate)	System capacity, TES C rate = -0.15 1/h

In addition to the no-shaving scheme with the same configuration, we also considered an air-source, non-cascaded heat pump with a backup electric heater as the second baseline. The non-cascaded heat pump is a basic 4-component configuration without thermal storage integration. The second baseline is used to calculate the peak reduction and energy saving potential against what may be installed today.

3. RESULTS AND DISCUSSION

3.1 System performance with and without peak shaving

This section compares the system performance using the two control strategies described in section 2.3. Figure 4a shows the heat transfer rates in the heating coil and the TES heat exchanger, and Figure 4b compares the electric power profiles of the high stage and low stage compressors with and without peak shaving. For both control schemes, the thermal storage device starts fully charged ($SOC = 100\%$). In the first case, where the system does not shift any energy, the TES discharging and charging heat transfer rates are equal and no net heat is extracted from the TES heat exchanger (net zero C-rate). The imposed building load profile and ambient temperature swing results in an approximately $2\times$ change in electric power throughout the day, with a peak power of 4.28 kW at 6:00 (Figure 4b).

The second control scheme utilizes the TES to reduce the heat supplied by the low stage circuit during the discharge window (TES charging heat transfer rate), lowering the refrigerant flow rate in this circuit. The mismatch between the discharging and charging heat rates is made up by the stored thermal energy in the TES heat exchanger. In Figure 4a, the area between the blue and red curves in the discharge window equals the TES storage capacity of 17.6 kWh. The reduced low stage capacity notably decreases the low stage compressor power throughout the discharge window, resulting in a 23.5% reduction in the peak power during this period. Once the TES is fully discharged, it remains at 0% state of charge until 14:00 when the system switches to the net-charging mode. In the charge window, the system increases the low stage compressor power so that the charging heat rate exceeds the discharging heat rate. As a result, a portion of the condensing heat rejected from the low-stage refrigerant goes towards melting (recharging) the PCM, while the remaining heat goes to the high stage refrigerant. Overall, the peak shaving control scheme substantially reduced the electric power during the discharge window at the cost of elevated power during the charge window.

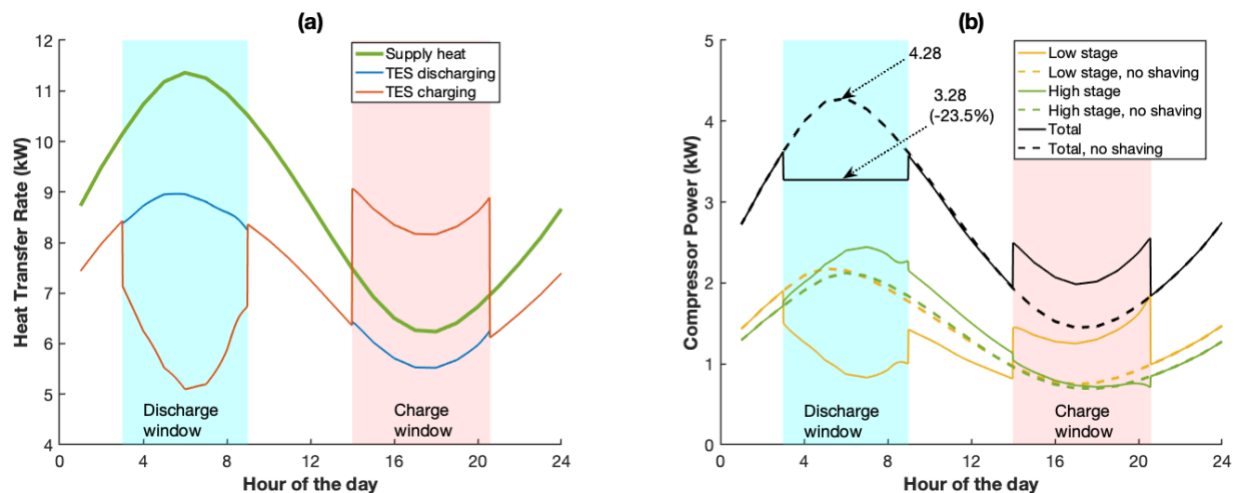


Figure 3: (a) Heat transfer rate supplied to the room and the heat transfer rates from the condensing (charging) and evaporating (discharging) streams in the TES heat exchanger, and (b) the individual and total compressor power profiles. The discharge and charge windows for the peak shaving control scheme are shown in blue and red panels, respectively. The peak electric power is reduced by 23.5% during the discharge window.

The compressor powers during the discharging and charging windows are a function of the refrigerant flow rate, compression ratio, and compressor isentropic efficiency. During the discharge window, the low stage heating capacity decreases, which reduces the refrigerant flow rate in the outdoor circuit. Since the heating coil must still provide the same room load, the evaporating refrigerant in the TES heat exchanger extracts the stored latent heat by freezing the

PCM, resulting in a net discharge of the TES. The transitioning region remains at 10 °C, but thermal resistances in the device increase as it discharges because a solid layer of PCM develops between the refrigerant channel and the transitioning region. As a result, the high stage evaporating dew point (T_{dew}), or the saturated vapor temperature in the high stage evaporator decreases as the state of charge drops, which also allows the low stage condensing T_{dew} to decrease and continue supplying heat to the boiling/evaporating stream (Figure 5a). Additionally, the low stage evaporating T_{dew} in the outdoor coil increases because less heat is transferred between the outdoor air and refrigerant, requiring a lower driving temperature difference. These temperature changes decrease the low stage compression ratio and increase the high stage compression ratio. The decrease in the low stage compression ratio results in an increase in the compressor isentropic efficiency (Figure 5b). Together the lower compression ratio (smaller enthalpy change across the compressor), lower refrigerant flow rate and higher efficiency all lead to decreased low-stage power consumption during the discharge window for the peak shaving control scheme. Conversely, the discharge process increases the high stage compression ratio, which reduces the isentropic efficiency and slightly raises the compressor power. During this period, the decrease in the low stage compressor power outweighs the increase in the high-stage power, resulting in a reduction in the total power consumption.

Similarly, the internal resistances in the TES heat exchanger and the relative heat transfer rates increase the condensing and evaporating T_{dew} during the charge window. Also, the elevated low stage circuit capacity increases the compressor speed and results in more mass flow rate in the circuit, pushing down the low stage evaporating T_{dew} in the outdoor coil. These trends force the low stage compressor to run at higher volumetric capacities and lower isentropic efficiencies, which both increase the power over the no peak shaving case.

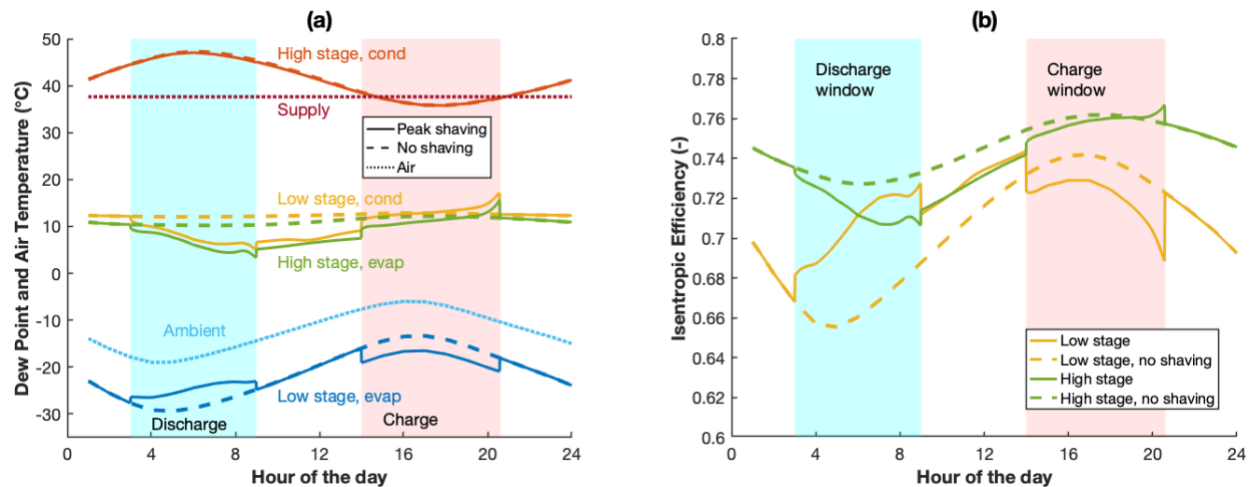


Figure 4: (a) System operating temperature profiles and the (b) compressor isentropic efficiency with and without peak shaving.

The peak shaving control scheme reduces the system energy consumption during the discharge window but increases the power consumption as the system recharges the TES to its full capacity during the charge window. The net energy saving could be a useful metric to compare to the peak shaving benefit. Figure 6 compares the electric energy consumption between the two control strategies. The peak shaving control scheme reduces the electric energy in the discharge window (3:00 – 9:00) by 4.5 kWh but increases the energy by 3.9 kWh to recharge TES in the charge window (14:00 – 20:40). Overall, the total net energy saving brought by peak shaving scheme is roughly 0.8 kWh (1.2% over the full day).

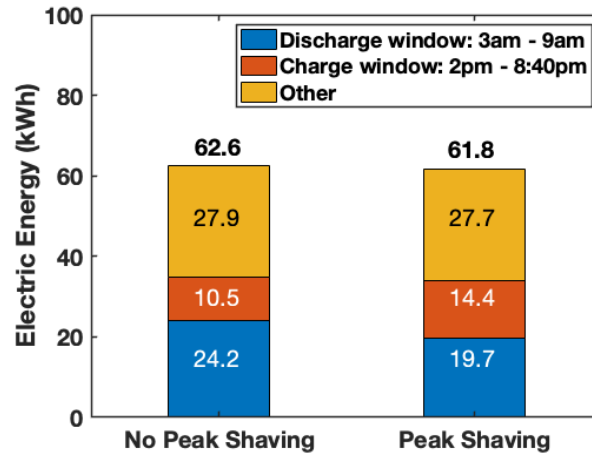


Figure 5: Electric energy consumption breakdown with and without peak shaving

3.2 Effect of TES transition temperature (T_t)

The PCM transition temperature is a critical design parameter for the proposed cascade system because it determines the intermediate operating temperatures (Low stage condensing T_{dew} and high stage evaporating T_{dew} in Figure 5a), which impacts the degree of energy saving that the system can provide with peak shaving scheme. When the transition temperature is 0 °C, the low-stage circuit consumes 11% of the total electrical power while providing the peak thermal load at 6:00. The thermal storage can reduce the low stage circuit capacity (and therefore the power consumption) as described above, but it will not have significant impact on the high stage electrical power which consumes most of the total power. Conversely, if the transition temperature is 20 °C, the low-stage circuit consumes 45% of the total power at 6:00. Therefore, using the thermal storage to drop the low-circuit capacity at a higher transition temperature has a more significant impact on the total energy saving, as shown in Figure 7, which shows the electric energy consumption saving or increase in comparison to the no shaving case at three different T_t : 0, 10, and 20 °C. Figure 7a shows that compared to the no shaving case, the system can shave more electric energy in the discharge window as the T_t increases. Meanwhile, as shown in Figure 7b, higher T_t requires more electric energy to recharge the TES component.

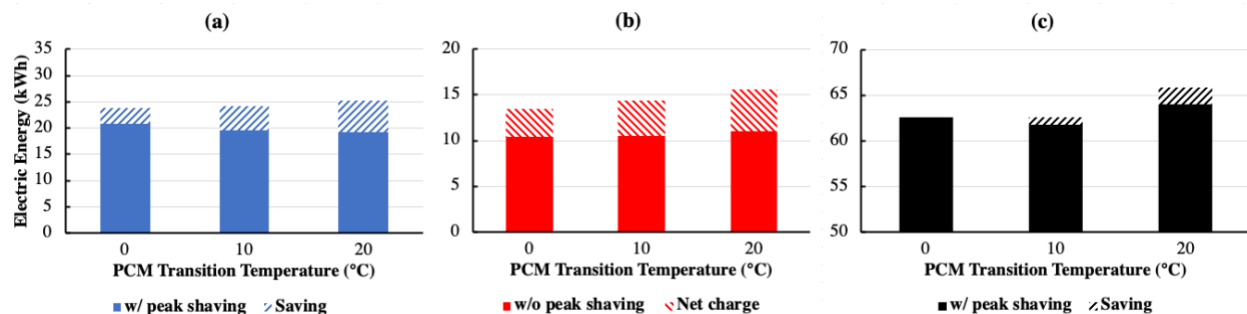


Figure 6: Electric energy consumption saving/increase in (a) discharge window: 3:00 – 9:00, (b) charge window: 14:00 – 20:40, (c) full day operation. The baseline for comparison is the same system without peak shaving. The shaded area in (a) indicates the saved energy during the discharge window. The shaded area in (b) is the extra energy required to charge TES. The shaded area in (c) is the net energy saving for the entire day operation.

Increasing T_t increases the compression ratio (and thus power consumption) for the low stage circuit but decreases the compression ratio for the high stage. However, Figure 7a and 7b show that the shaded area (energy saving or increase) grows monotonously as T_t increases from 0 to 20 °C. This is because discharging or recharging TES impacts the low stage performance more than the high stage. Taking the charge window for example, charging TES increases low stage circuit capacity compared to the no shaving case. This not only increases the compression ratio and reduces isentropic efficiency (which determines the enthalpy change in the compressor), but also increases the mass flow rate in the low stage circuit. On the other hand, charging TES does not significantly change the high stage mass flow rate,

because the high stage circuit operates at roughly the same capacity regardless of the low stage operation. While charging TES at elevated T_t decreases the compression ratio for the high stage, it increases both the compression ratio and mass flow rate for the low stage. Therefore, as T_t increases, the increase in low stage power consumption outweighs the decrease in high stage power in the charge window. Likewise, discharging TES lowers both compression ratio and mass flow rate for low stage. Therefore, increasing PCM T_t leads to more energy saving in the discharge window, and more energy consumption to recharge TES.

Figure 7c compares the total energy consumption with and without peak shaving. In the no-shaving case, the total energy consumption with the three T_t is 61.9, 62.6, and 65.8 kWh, respectively. As T_t increases, the low stage compression ratio increases while the high stage ratio decreases. Clearly, the increase in low stage power outweighs the saving in high stage power. With the peak shaving scheme, the total energy consumption becomes 62.6, 61.8, and 64.1 kWh, respectively. Figure 7c indicates that integrating PCM $T_t = 10$ °C leads to the least electric energy consumption with peak shaving. Overall, the net energy saving compared to the no shaving case is small (Figure 7c) regardless of PCM T_t .

Figure 8a shows peak reduction and energy saving at various T_t against the same system with no-shaving scheme. As discussed above, higher T_t gives more room for the TES to improve the low stage compressor performance during the discharge window. Thus, the peak electric power reduction increases from 17% to 28% as T_t increases from 0 to 20 °C. The net energy saving increases slightly from 1.3% to 2.6% as T_t goes from 10 to 20 °C. When $T_t = 0$ °C, the extra energy to recharge TES slightly exceeds the energy saved from the discharge window comparing to the no shaving case.

On the other hand, Figure 8b shows the load shifting benefit comparing to a typical air-source heat pump with a backup electric heater. When imposing the same load and ambient temperature profiles, this baseline air source heat pump operates with a peak electric power of 6.5 kW and consumes 113 kWh electric energy for the entire day. The baseline heat pump capacity drops as the ambient temperature decreases because the system is subjected to large compression ratio and thus suffers from significant throttling loss. Thus, we use the electric heater (COP = 1) to make up the difference between the system capacity and building thermal load. Therefore, the baseline heat pump peak power and electric energy consumption are both significantly higher than the proposed cascaded system which do not require back up electric heater. The peak electric power reduction increases from 46.1% to 50.9% as T_t increases from 0 to 20 °C. The energy saving in the discharge window increases from 44.9% to 49.1%. The net energy saving peaks when $T_t = 10$ °C at 45.5%. This is because integrating a PCM with $T_t = 10$ °C consumes the least energy with peak shaving operation, which is consistent with trend as shown in Figure 7c.

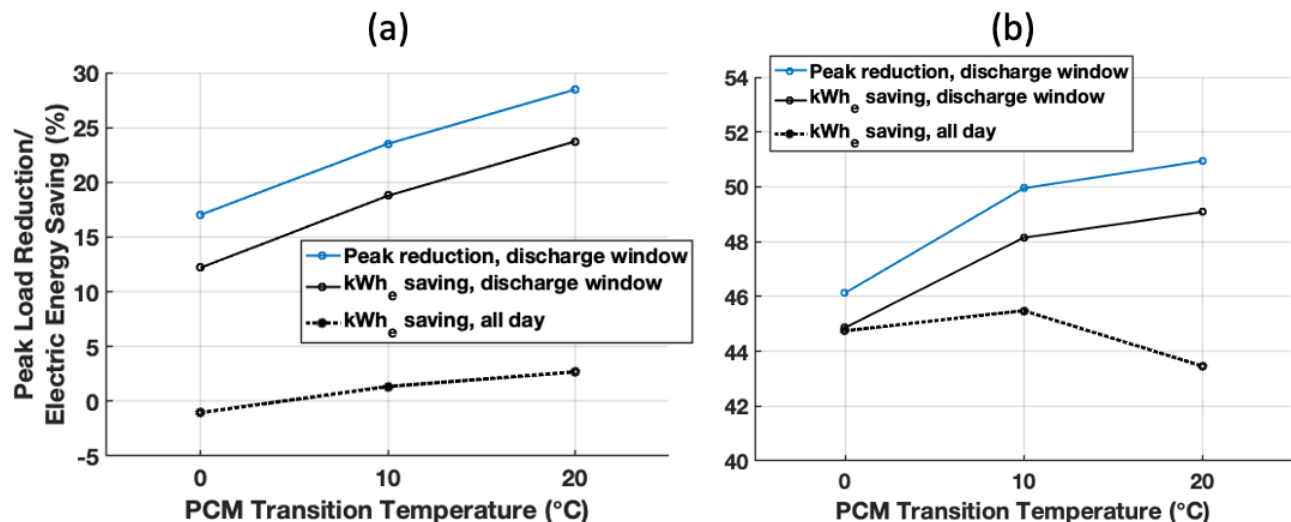


Figure 7: Peak reduction and energy saving as a function of PCM transition temperature comparing to (a) cascaded heat pump with no shaving case, (b) an air source heat pump with back up electric heater. The blue curve is the peak reduction, and the black curves are electric energy savings. The solid line indicates the reduction/saving in the discharge window (3:00 – 9:00), while the dotted line indicates the net saving for all day.

It should be noted that the results presented are based on the assumptions that compressor volumetric efficiency and isentropic efficiency are linear functions of only the compression ratio. Its deviation from characterizing the compressor with a performance map (e.g., 20 coefficient map) is that it does not capture the variance in isentropic efficiency at different RPM or different saturation dew point temperatures. The isentropic efficiency curve will be equipment specific. Based on our analysis of an off-the-shelf 20 coefficient performance map with the similar compressor inputs, the linear assumption notably over-predicts the low stage isentropic efficiency, and thus under-predicts the peak reduction and energy saving potential in the discharge window. Therefore, we believe that it is worthwhile to investigate the design of the proposed system with the appropriate compressor performance maps.

4. CONCLUSIONS

This study presented a novel cascaded heat pump system with integrated phase change thermal storage for the building electric peak load shaving. We simulated the load shifting performance of the system over a winter design day and investigated the effect of PCM T_t on the peak reductions and energy savings comparing to both the baseline operation (no peak shaving) and a baseline system (air-source heat pump with backup electric heater). Major conclusions are as follows:

- Peak shaving scheme effectively reduces the peak electric power consumption during the discharge window. For PCM $T_t = 10\text{ }^\circ\text{C}$, the TES reduces peak electric power by 23.5% compared to the no shaving scheme. The peak reduction is primarily due to smaller power consumption of the low stage compressor.
- The peak shaving scheme elevates the power consumption in the charge window. For PCM $T_t = 10\text{ }^\circ\text{C}$, the system saves 4.5 kWh during the discharge window but requires 3.8 kWh more energy to recharge TES heat exchanger. Overall, net energy saving of the peak shaving scheme is 0.8 kWh when comparing to the no shaving scheme.
- For the proposed system, discharging or recharging TES has a larger impact on the low stage circuit than the high stage. Therefore, PCM T_t impacts the load shifting characteristics of the proposed system. As T_t increases from 0 to 20 $^\circ\text{C}$, the peak reduction increases from 17% to 28%, and the energy saving in the discharge window increases from 12% to 24% comparing to the no shaving scheme.
- When comparing to an air-source heat pump with a backup electric heater, integrating PCM = 10 $^\circ\text{C}$ with peak shaving leads to 45.5% electric energy saving considering the full day operation, which is the highest among the three transition temperatures.
- The results assume that compressor efficiencies are linear functions of only the compression ratio. We believe that comparing to a compressor performance map that captures the variance of isentropic efficiency with RPM and saturation dew point temperature, the current assumption under-predicts the peak reduction and energy saving potential in the discharge window. The results are also dependent on ambient temperature profiles and the initial TES SOC of the day. We estimate that energy saving potential associated with peak shaving will decrease with a smaller temperature swing. And the peak power reduction achievable will decrease if TES is not fully charged at the start of the day.

NOMENCLATURE

HX	Heat exchanger	(-)
J	Junction	(-)
PCM	Phase change material	(-)
TES	Thermal energy storage	(-)
T_{dew}	Dew point temperature, or saturated vapor temperature	(K)
T_t	PCM Transition temperature	(K)
SOC	State of charge	(-)

REFERENCES

- Cooper, S., Hammond, G., McManus, M., & Danny, P. (2016). Detailed simulation of electrical demands due to nationwide adoption of heat pumps, taking account of renewable generation and mitigation. *IET Renewable Power Generation*, 10(3), 380-387.

- Dannis, J., & Schnabel, R. (1996). *Numerical methods for unconstrained optimization and nonlinear equations*. SIAM.
- Hirmiz, R., Teamah, H., Lightstone, M., & Cotton, J. (2020). Analytical and numerical sizing of phase change material thickness for rectangular encapsulations in hybrid thermal storage tanks for residential heat pump systems. *Applied Thermal Engineering*, 170, 114978.
- Huang, R., Aute, V., & Ling, J. (2021). A tripartite graph based methodology for steady-state solution of generalized multi-mode vapor compression systems. *Applied Thermal Engineering*, 116385.
- Huang, R., Ling, J., & Aute, V. (2020). Comparison of approximation-assisted heat exchanger models for steady-state simulation of vapor compression system. *Applied Thermal Engineering*, 166, 114691.
- Hutty, T., Patel, N., Dong, S., & Brown, S. (2020). Can thermal storage assist with the electrification of heat through peak shaving? *Energy Reports*, 6, 124-131.
- Hwang, Y. (2004). Potential energy benefits of integrated refrigeration system with microturbine and absorption chiller. *International Journal of Refrigeration*, 27(8), 816-829.
- Kuznik, F., Lopez, J., Baillis, D., & Johannes, K. (2015). Design of a PCM to air heat exchanger using dimensionless analysis: Application to electricity peak shaving in buildings. *Energy and Buildings*, 106, 65-73.
- Leung, J. (2018). *Decarbonizing US buildings*. Arlington: Center for Climate and Energy Solutions.
- Moreno, P., Sole, C., Castell, A., & Cabeza, L. (2014). The use of phase change materials in domestic heat pump and air-conditioning systems for short term storage: A review. *Renewable and Sustainable Energy Reviews*, 39, 1-13.
- Sharif, A., Al-Abidi, A., Mat, S., Sopian, K., Ruslan, M., Sulaiman, M., & Rosli, M. (2015). Review of the application of phase change material for heating and domestic hot water systems. *Renewable and Sustainable Energy Reviews*, 42, 557-568.
- Waite, M., & Modi, V. (2020). Electricity load implications of space heating decarbonization pathways. *Joule*, 4(2), 376-394.
- Woods, J., Mahvi, A., Goyal, A., Kozubal, E., Odukamaiya, W., & Jackson, R. (2021). Rate Capability and Ragone Plots for Phase Change Thermal Energy Storage. *Nature Energy*, 6(3), 295-302.

ACKNOWLEDGEMENT

This work was authored by the National Renewable Energy Laboratory, operated by Alliance for Sustainable Energy, LLC, for the U.S. Department of Energy (DOE) under Contract No. DE-AC36-08GO28308. Funding provided by the U.S. Department of Energy Office of Energy Efficiency and Renewable Energy Building Technologies Office. The views expressed in the article do not necessarily represent the views of the DOE or the U.S. Government. The U.S. Government retains and the publisher, by accepting the article for publication, acknowledges that the U.S. Government retains a nonexclusive, paid-up, irrevocable, worldwide license to publish or reproduce the published form of this work or allow others to do so, for U.S. Government purposes.